ORIGINAL ARTICLE

Web-based bone age assessment by content-based image retrieval for case-based reasoning

Benedikt Fischer · Petra Welter · Rolf W. Günther · Thomas M. Deserno

Abstract

Purpose Maturity estimation by radiological bone age assessment (BAA) is a frequent task for pediatric radiologists. Following Greulich and Pyle, all hand bones are compared with a standard atlas, or a subset of bones is examined according to Tanner and Whitehouse. We support BAA comparing the epiphyses of a current case to similar cases with validated bone age by content-based image retrieval (CBIR).
Methods A web-based prototype case-based retrieval system for BAA was developed and is publicly available. Hand radiographs from the USC database or user uploads may be retrieved by image-based query. The ten best matching cases for each epiphysis are retrieved by CBIR and displayed with their BAA, similarity score, and the derived age estimate. The similarity is approximated by cross-correlation. The USC hand database includes 1,101 cases comprising four ethnic groups of both genders between zero and 18 years of chronological age with radiographs and two annotated BAA. The USC image data have been enriched by marking the epiphyseal centers between metacarpals and distal phalanges.
Results Leave-one-out experiments yielded a mean error rate of 0.99 years and a standard deviation of 0.76 years in comparison with the mean USC–BAA. The research prototype enables radiologists to judge their agreement based on similarity of retrieved cases and the derived age.

Conclusions CBIR provides support to the radiologist with a second opinion for BAA. Self-explanatory web applications can be established to support workflow integration. Enhancements in similarity computation and interface usability may further improve the system.

Keywords Radiography · Image processing · Computer-aided diagnosis (CAD) · Bone age assessment (BAA) · Content-based image retrieval (CBIR) · Case-based reasoning (CBR)

B. Fischer (✉) · P. Welter · T. M. Deserno
Department of Medical Informatics, RWTH Aachen University,
Pauwels str. 30, 52057 Aachen, Germany
e-mail: bfischer@mi.rwth-aachen.de

T. M. Deserno
e-mail: tdeserno@mi.rwth-aachen.de

R. W. Günther
Department of Diagnostic Radiology, University Hospital Aachen,
Pauwels str. 30, 52057 Aachen, Germany

Abbreviations

BAA	Bone age assessment
CAD	Computer-aided diagnosis
CARS	Computer-assisted radiology and surgery
CBIR	Content-based image retrieval
CBR	Case-based reasoning
CLEF	Cross-language evaluation forum
CCF	Cross-correlation function
eROI	Epiphyseal region of interest
GUI	Graphical user interface
GP	Greulich and Pyle
IDM	Iterative distortion model
ImageCLEF	Image retrieval track of the cross-language evaluation forum
IRMA	Image retrieval in medical applications
PACS	Picture archiving and communication system
QBE	Query-by-example
RIS	Radiological information system
ROI	Region of interest
TW2/TW3	Bone age ratings by Tanner and Whitehouse
USC	University of Southern California

Introduction

The determination of skeletal maturity, also referred to as bone age assessment (BAA), is usually based on hand radiographs and constitutes a frequent and mostly time-consuming task in radiological routine. Relating bone to chronological ages and the current status of growth allows to estimate the adult height of pediatric subjects, as well as to diagnose and track endocrine disorders or pediatric syndromes [1,2]. Under certain conditions, BAA may also contribute to forensic age diagnostics of adolescents and young adults [3,4].

In general, the bone age is determined manually from the visual comparison of the patient's hand radiograph to a standardized atlas. Clinically, the methods by Greulich and Pyle [5] or Tanner and Whitehouse [6] are applied. In order to reduce the manual effort, several approaches using digital image processing have been published for (semi-)automatic measurements [7–14].

However, any measurement on the bones relies on the successful localization and delineation of the bone segments. Yet particularly in the medical domain, automatic segmentation is known to be error-prone, requiring manual interaction [15]. Concerning skeletal radiography of hands, the summation effect, i.e., the projection of the three-dimensional (3D) structures into a two-dimensional (2D) image, results in over-segmentation, especially for the lower end of the metacarpal and carpal bones. In addition, varying radiation dose and noise worsen the delineation of relevant bones. Even within a certain reference group of the GP atlas, substantial differences of the bone segments exist [1,5]. In combination with many different poses, this aggravates the development of model-based segmentation methods, which have been applied successfully in many applications of medical imaging [16].

We therefore omit measurements relying on exact delineation. Instead, we aim at mimicking the human concept of visual comparison with past cases, merging the popular approaches of case-based reasoning (CBR) [17] with content-based image retrieval (CBIR) [18,19]. In order to stir the scientific discussion on combined CBR/CBIR for BAA, we set up a web interface that is publicly available. In contrast to black-box solutions that only display the result, this interface explicitly displays the cases considered most similar, providing relevance facts to the user on how the stated bone age has been derived.

Methods

Bone age assessment

The CBR paradigm is intended to simulate the human problem-solving behavior for new problems by compari-

son to already experienced problems [17]. In the medical domain, it has successfully been applied for decision support in educational contexts [20]. CBIR-supporting CBR has come to attention for medical applications, particularly in radiology [18,19]. With the entailed Query-by-example (QBE) approach, CBIR is a straightforward application of CBR regarding images, where similar images of previous cases are retrieved from a database in order to solve the given task for the query image.

In our system, not only images but also validated case information such as chronological age, ethnic origin, gender, and multiple bone age readings are collected, building an extensible set of ground truth data. This information can be used directly to support decision making. If the newly solved cases are added to the case database, the complete CBR cycle (retrieve–reuse–revise–retain) can be applied as specified by Aamodt and Plaza [17]. In the current environment, we have focused on the retrieval and reuse phases. For this, we utilized the Image Retrieval in Medical Applications (IRMA) framework supporting image retrieval, large scale experiments, and validation processes [21,22].

For the specific application to BAA, we specialized the framework to retrieve regions of interest (ROI) similar to those of a given hand radiograph rather than using the global similarity between complete images as used for example in the ImageCLEF contests [23]. A similar approach has been introduced by Tanner and Gibbons, where manually extracted regions of interest from secondary digitization are compared by Fourier coefficients [13]. In general, the epiphyseal regions of interest (eROI) reliably indicate the bone age (Fig. 1), especially in the range of bone ages between 2 and 18 years [1,12,24].

The complete processing pipeline encompasses the following steps (Fig. 2):

- center localization of the eROIs,
- normalized region extraction of the eROIs,
- case-based comparison using a CBIR engine, and
- age assessment computing the overall bone age estimation from the ground truth associated with each retrieved eROI.

Center localization

In order to obtain comparable image patches for CBR, each eROI is extracted in a standardized way. The eROI centers can be either computed fully automatically [25] or located interactively: At first, the positions of the topmost fingertip and the top of the ulna are marked to ensure comparable scaling independent of the provided image resolution. In the next step, the centers of relevant eROIs are localized by corresponding mouse clicks. Up to 19 eROIs may be used for

Fig. 1 Successive stages of skeletal development of healthy male subjects. The radiographs have been acquired at the University Hospital Aachen, Germany
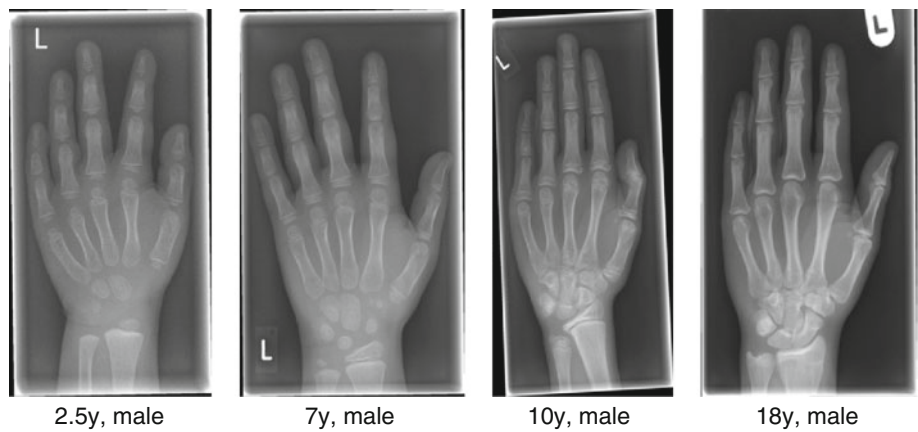

| 2.5y, male | 7y, male | 10y, male | 18y, male |

Fig. 2 Successive stages of CBIR-assisted BAA. Query and reference data (ground truth) are marked in *green* and *red*, respectively
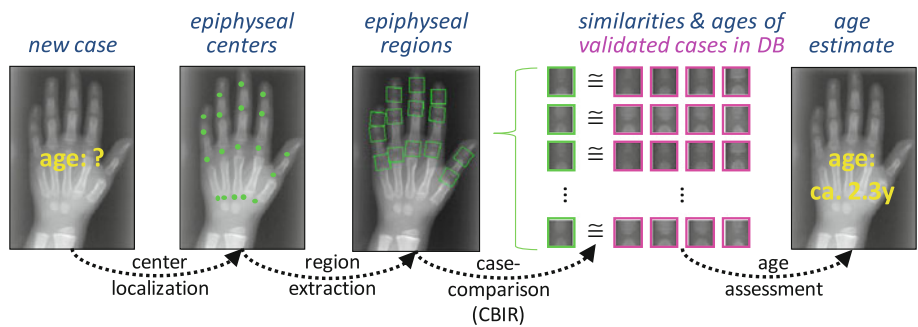

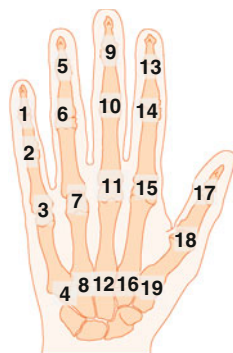**Fig. 3** Assigned labels for the eROI positions

Fig. 4 eROI extraction. The orientation for eROI no. 18 (*solid line*) is set to the mean of the connecting axes to eROI no. 17 (*dashed*) and no. 19 (*dotted*)

BAA (Fig. 3). In accordance with restrictions of the automatic eROI extraction algorithm, only the 14 eROIs between metacarpals and upper phalanx are used for the age estimation. In other words, eROIs 4, 8, 12, 16, and 19 are disregarded in further processing.

After that, the complete bone age determination process is performed fully automatically.

Region extraction

The size is computed by scaling the bounding box to the size corresponding to 25×30 pixels if the image between the two marked positions was scaled aspect preserving to 256 pixels height. This size has been proven successful in earlier experiments [24]. The orientation of the bounding boxes is determined by the mean of the straight lines connecting the current eROI center to the centers of eROIs above and below (Fig. 4). If only one neighboring eROI center is present, the eROI orientation is set to the straight line connecting this neighbor.

Case comparison using a CBIR engine

For each extracted eROI, an individual query is performed. Each patch is submitted to the CBIR engine in a separate run. The CBIR engine compares each submitted eROI to all eROIs in the database that have been extracted from the same position. Technically, only eROIs of the same label are compared, so that, e.g., the epiphysis of the distal phalanx of the middle finger is only compared with epiphyses of distal phalanges of other middle fingers and not, for example, to epiphyses of proximal phalanges.

Table 1 Categories and corresponding number of samples per year in the USC hand atlas

Age group/Ethnics-gender	AS-F	AS-M	AA-F	AA-M	CA-F	CA-M	HI-F	HI-M
<1 year	1	2	4	5	3	3	1	5
1–9 years (each)	5	5	5	5	5	5	5	5
10–18 years (each)	10	10	10	10	10	10	10	10

Ethnic origin is encoded as *AS* Asian, *AA* African American, *CA* Caucasian, *HI* Hispanic; Gender: *F* Female, *M* Male [26]

An eROI e is represented as a two-dimensional matrix, where an entry $e(x, y)$ represents the intensity of the pixel at position (x, y) within the extracted region of interest. The similarity between two eROIs e and p of the dimensions $X \cdot Y$ is measured by the cross-correlation function (CCF):

$$D_{\text{CCF}}(e, p) = \max_{|m|, |n| \leq d} \left\{ \frac{\sum_{x=1}^{X} \sum_{y=1}^{Y} ((p(x - m, y - n) - \bar{p})(e(x, y) - \bar{e}))}{\sqrt{\left(\sum_{x=1}^{X} \sum_{y=1}^{Y} (p(x - m, y - n) - \bar{p})^2\right) \cdot \left(\sum_{x=1}^{X} \sum_{y=1}^{Y} (e(x, y) - \bar{e})^2\right)}} \right. \tag{1}$$

The variables $\bar{p}$ and $\bar{e}$ denote the respective mean intensity values of p and e, while d is the warp range of the correlation.

While the CCF may be regarded as a relatively simple measure, it provides a direct comparison of the image pattern and comes with an important benefit for handling radiological images: it is robust against the radiation dose, which is normalized by subtracting $\bar{p}$ and $\bar{e}$.

For an age estimation involving r epiphyses, r queries to the CBIR engine are submitted. For each submission, the CBIR engine returns a sorted list of the K most similar eROIs together with their respective similarity and validated bone age. The similarity scoring for the kth-similar eROI, $1 \leq k \leq K$, to the rth query eROI is provided by the sorted list $\partial(r, k)$, the corresponding age by $a^{\text{known}}(r, k)$.

Age assessment

There are many options for combining the ground truth metadata of similar images to estimate a reliable guess of the bone age. In our definition, we want to combine the following aspects:

- Each retrieved eROI is weighted by its similarity to the query eROI. The more similar, the more influence on the age estimation is gained.
- Each eROI position is weighted identically by $1/R$. This allows the estimation of the bone age of each individual eROI position and the overall bone age assessment in a final procedure.

From the similarities and known ages of the retrieved previous cases' eROIs, the bone age estimation for each eROI position r and the complete hand h of the current case is derived accordingly:

$$a^{\text{predict}}(h) = \frac{1}{R} \sum_{r=1}^{R} \left(\frac{1}{\sum_{k=1}^{K} \partial(r, k)} \sum_{k=1}^{K} a^{\text{known}}(r, k) \partial(r, k) \right) \tag{2}$$

Case database for retrieval

The University of Southern California (USC) has provided a digital hand atlas [11] of 1,103 radiographs attributed with two bone age readings by experienced radiologists. The radiographs are categorized by chronological age, gender, and ethnics as shown in Table 1. The downloadable atlas contained a corrupted image and for one case of a 14-year-old Caucasian female, both reference readings had entries of 99.99 years. Excluding both cases yielded 1,101 reference radiographs remaining. For automatic processing, we defined the mean of the two reference readings as ground truth for each of the cases.

Evaluation

The prediction quality of our CBIR-based BAA system is measured by the mean μ and the standard deviation σ of the absolute difference between the predicted age $a^{\text{predict}}(h)$ and the average of the two radiologists' readings ($a^{\text{read1}}(h)$ and $a^{\text{read2}}(h)$, respectively) recorded in the USC database for each hand h:

$$\mu_{\text{err}} = \frac{1}{H} \sum_{h=1}^{H} \left| \frac{a^{\text{read1}}(h) + a^{\text{read2}}(h)}{2} - a^{\text{predict}}(h) \right|$$

$$\sigma_{\text{err}} = \sqrt{\frac{1}{H}\sum_{h=1}^{H}\left(\left|\frac{a^{\text{read1}}(h)+a^{\text{read2}}(h)}{2}-a^{\text{predict}}(h)\right|-\mu_{\text{err}}\right)^2}$$

(3)

Here, H denotes the number of hand radiographs. Concerning the similarity computation D_{CCF}, we use 16×16 scaled versions of the eROIs, i.e., $X = Y = 16$, and a warp range of $d = 2$ to determine the maximum correlation.

In the experiments, the overall prediction quality and the influences of the number of eROIs R as well as the number of considered most similar neighbors K of a query eROI are analyzed. Since at most 10 radiographs in the USC hand atlas belong to the same group concerning age, gender, and ethnic origin, K is considered only for values from 1 to 10.

In order to avoid computation of all possible 2^{14} set combinations for the 14 eROIs, we performed a three stage evaluation concept:

1. The performance of each eROI position is assessed individually. According to Tanner and Whitehouse, some eROIs are more reliable for BAA than others. Accordingly, $R = 1$.
2. The seven individually best eROIs are combined and analyzed as a set ($R = 7$), i.e., half of all available eROIs.
3. The full set of all eROIs ($R = 14$) is used.

All experiments are performed in leaving-one-out runs.

Web-based user interface

The lack of appropriate user interfaces that integrate computer-aided diagnosis (CAD) into the clinical workflow in a hospital's department of radiology is termed the "application gap" [27]. Other investigations have shown that physicians prefer web search engines and web-based interfaces to retrieve interesting image data from archives [28,29].

Therefore, we aimed at developing a web interface for BAA that further narrows the application gap. It shall feature two operating modes:

- In "demonstration mode" the user may browse through available radiographs from the reference database prior to selecting one, which is then analyzed using the remaining ground truth data.
- In "local mode", the user can upload an appropriate radiograph from her local system to the web server and a BAA guess is returned as a second opinion. For this, she needs to set manually the required landmarks as described in section "Center localization". Again, the USC data are used as ground truth.

An overview of the complete web-based scenario is illustrated in Fig. 5. For implementation, we used the IRMA framework [21–23]. This provides Smarty templates for web-based GUI design and a large functionality for extended query refinement and relevance feedback including complete query logging of all user/system interaction [30]. PHP is used to interface a PostgreSQL database with an Apache web server on a Linux-based server PC running a 64bit Debian Linux. The current installation is available by internet and aimed at the scientific community. If a RIS/PACS integration is desired, the systems can also be setup in a hospital's internal network. A seamless integration into the radiological information systems (RIS) can then be achieved via DICOM Application Hosting and DICOM Structured Reporting [31,32]. The PACS database could be used as a steadily growing case database instead of the USC hand atlas and would complete the CBR cycle by adding the revise and retain phases.

Results

Validation experiments

To judge the prediction potential of individual eROIs, quality measures were obtained for each eROI and all $k = 1, \ldots, 10$. The results show mean absolute error rates between 1.04 and 1.87 years and minimum standard deviations between 0.76 and 1.58 (Table 2). The most reliable individual eROI is the proximal eROI of the middle finger (eROI no. 11 in Fig. 3), followed by the other proximal eROIs (no. 15, 7, 18, and 3 in Fig. 3). In general, the ranking degrades in the distal and less central directions.

The best single eROI (number 11 in Fig. 3), the best seven eROIs (numbers 11, 15, 7, 18, 3, 10, and 6 in Fig. 3), i.e., half of all eROIs, and the set of all eROIs have been subjected to increasing K (Table 3). The best mean error of 0.99 years is obtained by the set of 7 eROIs with a standard deviation of 0.79 for $K = 2$. The best standard deviation of 0.76 is achieved by the single eROI with a mean error of 1.04 years for $K = 10$. For $K = 2$ and 7 eROIs, the results in terms of sample size, observed absolute errors as mean, minimum, maximum, as well as standard deviation are provided for each age in Table 4. The required average runtimes were 2.84, 20.64, and 41.8 s for the single eROI, the "best seven" set and the complete set, respectively. These were obtained on a PC with an Intel® Xeon® CPU at 2.66 GHz.

Web-based user interface

The research prototype has been made publicly available.[1] Figure 6 shows a screen shot when selecting a query

---

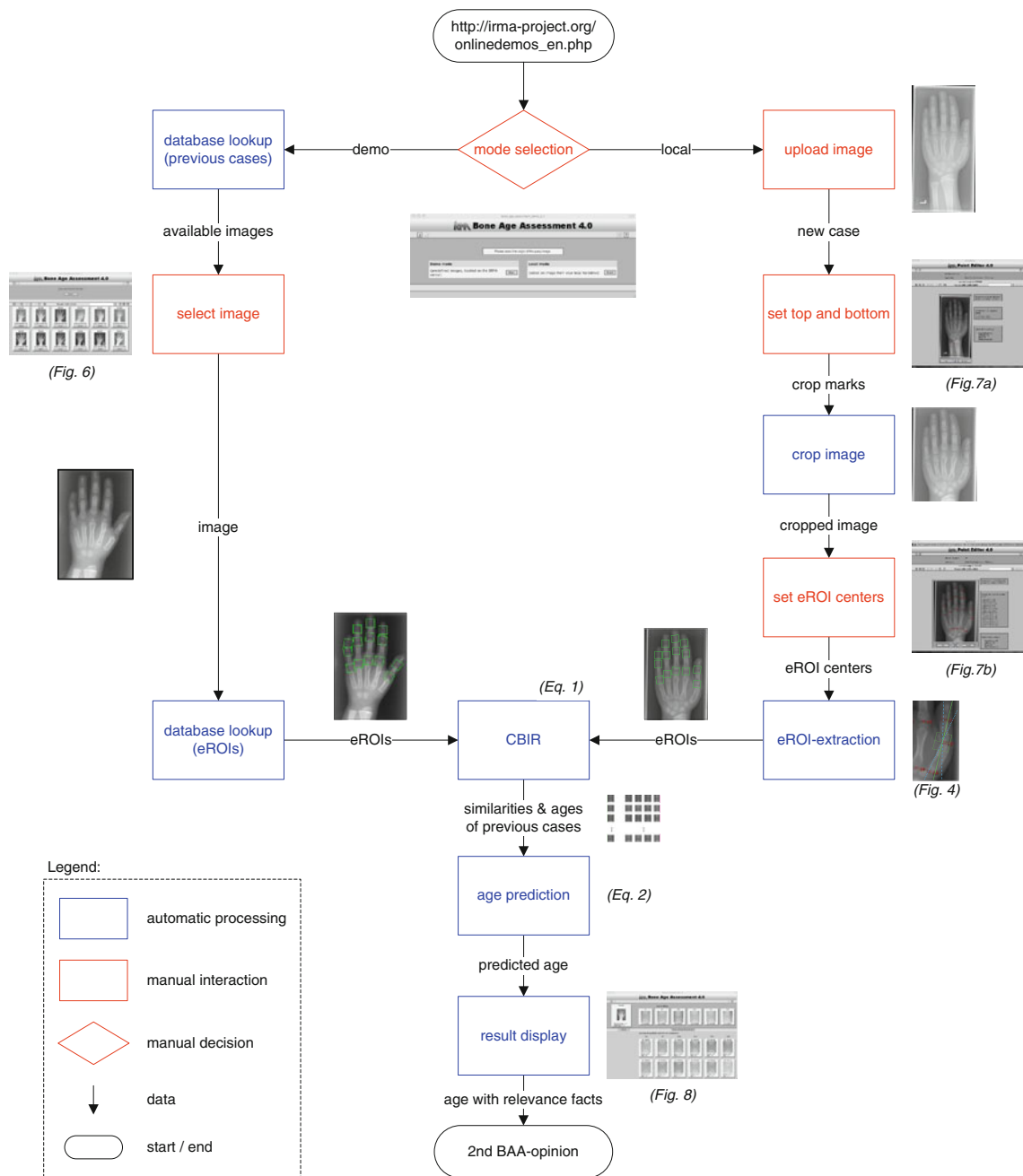[1] http://irma-project.org/onlinedemos_en.php.

Fig. 5 Complete processing pipeline for the web-based BAA; both modes compute similarities to the cases of the USC hand atlas

image in "demonstration mode". According to the general style of IRMA web interfaces, the graphical user interface (GUI) is partitioned vertically into distinct sections such as header bar, parameter field, status and navigation bar, and output field, where the icons of available images are displayed [30].

In the local mode, the user is not restricted to the cases of the USC hand atlas, but may choose an arbitrary image from a local resource. After uploading it and setting the top and bottom points to the topmost fingertip and the top of

the ulna (Fig. 7a), respectively, the image is cropped and the eROI centers can be located by the user. The marked points are numbered consecutively and can be corrected in their position, removed, and re-inserted (Fig. 7b). The numbering scheme is displayed to the user in a separate window (not shown).

After the user submits the center positions by clicking on the OK button, all eROIs are extracted automatically and the CBIR query is performed on the data of the USC hand atlas by the IRMA system.

Table 2 Best results for individual eROIs

	eROI	1	2	3	5	6	7	9	10	11	13	14	15	17	18	Min	Max	Mean
Min-mean	Min-mean	1.87	1.63	1.30	1.65	1.40	1.17	1.53	1.34	**1.04**	1.59	1.41	1.07	1.64	1.29	1.04	1.87	1.42
	K	5	6	9	4	8	10	10	7	10	5	7	9	5	10	4	10	8
	Ranking	14	11	5	13	7	3	9	6	1	10	8	2	12	4			
Min-SD	Min-SD	1.58	1.28	0.96	1.37	1.16	0.85	1.35	1.11	**0.76**	1.40	1.11	0.83	1.39	1.00	0.76	1.58	1.15
	K	5	6	7	7	9	10	10	9	10	5	5	10	10	10	5	10	8
	Ranking	14	9	4	11	8	3	10	7	1	13	6	2	12	5			

For each eROI, the observed minimum mean absolute prediction error and the minimum standard deviation are provided with the corresponding number of retrieved eROIs, K. The ranking provides an alternative ordering by the quality measures instead of the eROI number. The best results are in bold

Table 3 Set performances for increasing number of retrieved eROIs K

	K	1	2	3	4	5	6	7	8	9	10	Min	Max	Mean
Best eROI (no.11, Fig. 3)	Mean	1.40	1.20	1.12	1.09	1.08	1.05	1.05	1.05	**1.04**	1.04	1.04	1.40	1.11
	SD	1.16	0.96	0.91	0.86	0.84	0.80	0.80	0.78	0.77	0.76	0.76	1.16	0.87
7 Best eROIs	Mean	1.02	**0.99**	1.00	1.01	1.03	1.03	1.04	1.05	1.05	1.06	0.99	1.06	1.03
	SD	0.85	0.79	0.80	0.79	0.77	0.77	0.77	0.77	0.77	0.78	0.77	0.85	0.79
All eROIs	Mean	**1.08**	**1.08**	1.10	1.13	1.14	1.16	1.18	1.19	1.20	1.21	1.08	1.21	1.15
	SD	0.88	0.86	0.87	0.88	0.87	0.88	0.89	0.90	0.91	0.92	0.86	0.92	0.89

The best mean error for each set is in bold

Table 4 Mean absolute error for the 7 best eROIs with $K = 2$ for bone ages 1–18

Age	<1	1	2	3	4	5	6	7	8	9	10	11	12	13	14	15	16	17	18
Samples	23	40	40	40	40	40	41	40	40	40	80	79	80	80	80	79	80	79	80
Mean	0.99	0.79	0.75	1.06	1.00	1.03	1.09	1.28	1.12	1.13	1.13	1.04	0.99	1.03	0.94	0.83	0.66	0.93	0.99
Min	0.26	0.09	0.01	0.03	0.06	0.12	0.02	0.02	0.00	0.05	0.02	0.01	0.04	0.01	0.01	0.03	0.00	0.00	0.04
Max	1.59	2.98	2.23	3.12	3.28	3.29	3.00	3.63	2.86	3.53	2.82	2.94	3.33	2.75	3.00	2.28	2.45	3.08	2.90
SD	0.41	0.62	0.53	0.80	0.72	0.79	0.84	0.88	0.89	0.86	0.70	0.82	0.81	0.75	0.73	0.57	0.50	0.65	0.71

In both operating modes, the result is displayed with the original image and the extracted eROIs at the top with the K most similar eROIs for each extracted eROI shown below in decreasing order of similarity (Fig. 8). For ease of use, the number of retrieved most similar eROIs has been preset to $K = 10$. The number of eROI positions is preselected to seven (eROI no. 11, 15, 7, 18, 3, 10, and 6 in Fig. 3), in order to fit into the typical display resolution of 1,280 pixels width and as these provided the best results in the experiments.

For each retrieved eROI, the computed similarity to the query eROI as well as the validated bone age is shown. Each column corresponds to one eROI position. The query eROI is shown at the top and in the rows below the retrieved eROIs

are sorted by decreasing similarity. For better orientation, the corresponding eROI position is indicated in the query hand radiograph if the user moves the mouse over a query eROI (Fig. 9).

The overall bone age estimation is stated below the query image (Fig. 8). In the demonstration mode, the validated bone age from the USC atlas is additionally shown below the system's age estimation.

Each image may be clicked onto to open up a new window displaying the radiograph at its original resolution to allow a closer inspection. If desired, the user may also switch the display mode to show the hands belonging to the retrieved eROIs instead of the eROIs themselves (Button "Show corresponding hands" in Figs. 8 and 9).

Fig. 6 Example screen for browsing the available database before selecting an image for analysis. A detailed view of a hand radiograph is available by clicking on the thumbnails
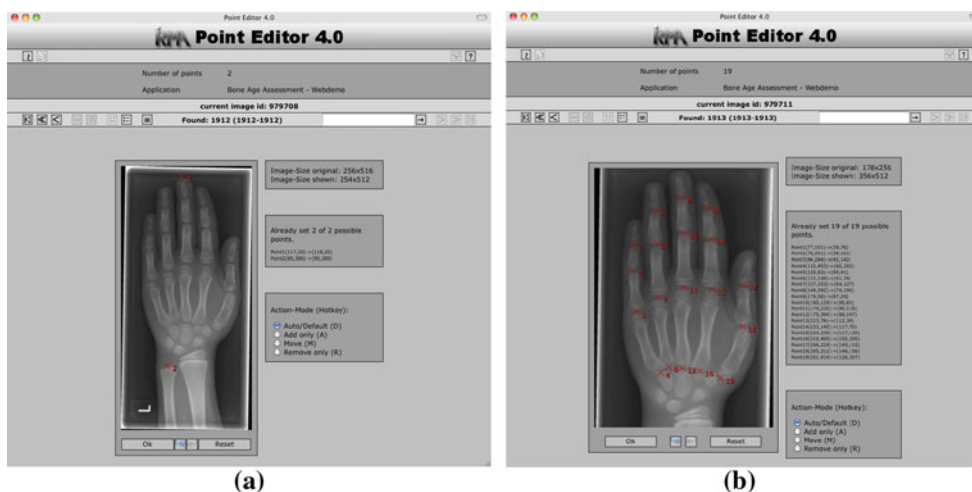

Fig. 7 Point Editor interface for setting the top and bottom crop marks (**a**) and labeling the epiphyseal centers (**b**)

Discussion

The aim of our work is twofold: First of all, we intend to establish a public web interface for BAA by CBIR-supported CBR to invite researchers and radiologists to test our prototype and provide feedback for further improvement. Second of all, we aim at assessing the prediction quality of the research prototype based on the USC hand atlas [11]. This reference is also used for the web-based BAA of radiographs uploaded by users.

We regard the first aim as achieved. However, the first prototype comes with a few limitations. So far, only images in DICOM or PNG format of at least 256 pixels in each dimension can be handled. The number of required mouse clicks and the number of pop-up windows will have to be decreased in order to improve the GUI usability. However, the prototype enables the radiologist to easily overview the most similar retrieved eROIs. We see this as a major advantage of our solution as important relevance facts are provided [30]. Possible pitfalls of a black-box CAD solution are avoided, by
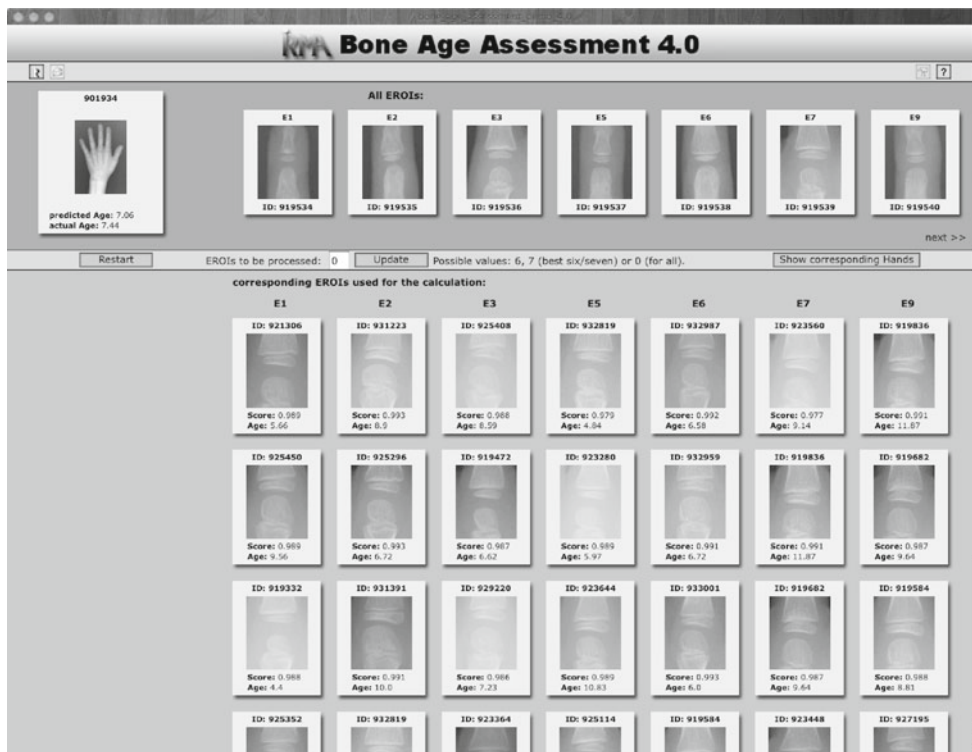
Fig. 8 Result display in demonstration mode for a screen that fits seven eROIs. Query image and extracted eROIs are shown at the *top*. Their most similar counterparts retrieved from the database are shown *below* (scrollable) in decreasing similarity and with the previously diagnosed bone age. The estimated and the validated bone age are shown *right* below the query image. In the local mode with a newly uploaded image, the known bone age is not available
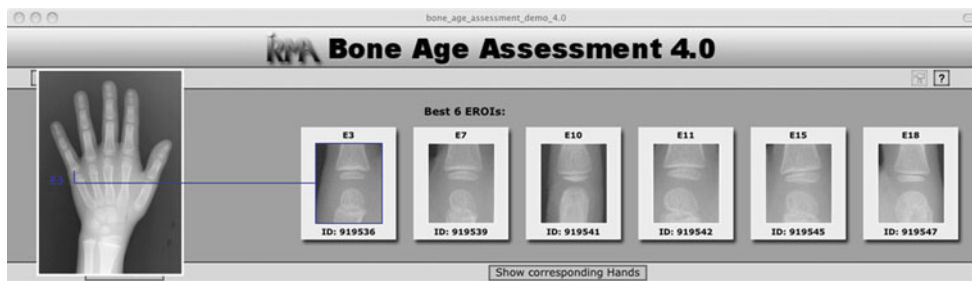

Fig. 9 A mouse-over effect for the extracted eROIs illustrates their position in the radiograph (topsection of the result display)

explicitly presenting the radiologist how the results have been obtained. With the additional information, the radiologist is assisted in drawing own conclusions on account of similar cases that are directly linked to the appropriate images for each eROI.

Regarding our second aim, the observed evaluation results with a mean absolute error of roughly one year with a standard deviation of about 0.8 are considered as good first results, keeping in mind that also images of patients below 2 years and above 15 are included and that we have not distinguished between genders or ethnic origins. In the commercial application BoneXpert,[2] which can be considered the best solution published, bone ages are estimated with certainty only within the range of 2.5–17 and 2–15 years for boys and girls, respectively [12]. With these limitations, they obtain a root mean square error of 0.61 years. The comparison with further approaches including [13] is ambiguous due to the use of non-public datasets, different age or ethnic groups, error measures, or differing bone age ratings such as TW2/TW3. Using the publicly available USC hand atlas and by providing a public web interface, we aim at facilitating future comparisons in the field.

---

[2] http://www.bonexpert.com.

The computational runtimes of our system can be regarded as sufficiently fast to be accepted by radiologists. The results especially for the 7 best eROIs provide a reasonable compromise between assessment precision and runtime. Using only a single eROI obtains sufficient reliability but additional eROIs increase robustness.

Future work will concentrate on improvements of the similarity computation, web site usability, and comprehensive validation. The similarity computation will be enhanced by comparing eROIs only within the same gender and by additional image features such as Tamura features and iterative distortion model (IDM) [21].

The inclusion of the carpal bones as well as the distal radius and ulna is expected to additionally enhance the assessment quality. Furthermore, we aim at developing prototypes that represent certain classes of age, gender, and ethnics. To improve the usability of the web interface, we will decrease the required number of mouse clicks and include relevance feedback allowing the users to (de)select or weight the retrieved eROIs for inclusion in the age computation. The automatic localization of the eROIs will be enhanced by the Generalized Hough Transform as used in [14,33]. A comprehensive validation study is planned using 1,000 hand radiographs acquired and diagnosed in daily routine at the University Hospital Aachen, Germany. Variety in appearance, x-ray parameterization, aperture, pose, and artifacts is expected much higher when images are not acquired particularly for use in a reference atlas.

Conclusions

The validation experiments on the USC hand atlas indicate a robust bone age estimation, with a mean error below one year over all age groups.

The public web interface allows an independent judgment of our achievements as interested users may upload their own images for bone age estimation, yet any diagnostic use is explicitly excluded. Feedback on the CBIR approach and an exchange of ideas how to further enhance the system are encouraged.

Conflict of interest None.

References

1. Gilsanz V, Ratib O (2005) Hand bone age. a digital atlas of skeletal maturity. Springer, Berlin
2. Thodberg HH (2009) An automated method for determination of bone age. J Clin Endocrinol Metabol 94(7):2239–2244
3. Schmeling A, Lockemann U, Olze A et al (2004) Forensische Altersdiagnostik bei Jugendlichen und jungen Erwachsenen. Dtsch Arztebl 101(18)
4. Schmitt R, Lanz U (2008) Diagnostic imaging of the hand. Thieme Publishing Group, Stuttgart, p 148
5. Greulich WW, Pyle SI (1971) Radiographic atlas of skeletal development of hand wrist. Stanford University Press, California
6. Tanner JM, Healy MRJ, Goldstein H, Cameron N (2001) Assessment of skeletal maturity and prediction of adult height (TW3). WB Saunders, London
7. Wastl S, Dickhaus H (1996) Computerized classification of maturity stages of hand bones of children and juveniles. Engineering in Medicine and Biology Society, 1996. Bridging Disciplines for Biomedicine. In: Proceedings of 18th annual international conference IEEE, vol 3, pp 1155–1156
8. Martin-Fernandez MA, Martin-Fernandez M, Alberola-Lopez C (2003) Automatic bone age assessment: a registration approach. In: Proceedings of SPIE, vol 5032, pp 1765–1776
9. Pietka E, Gertych A, Pospiech S et al (2001) Computer-assisted bone age assessment: Image preprocessing and epiphyseal/ metaphyseal ROI extraction. IEEE Trans Med Imaging 20(8): 715–729
10. Park KH, Lee JM, Kim WY (2007) Robust epiphyseal extraction method based on horizontal profile analysis of finger images. In: Proceedings of ISITC, pp 278–282
11. Gertych A, Zhang A, Sayre J et al (2007) Bone age assessment of children using a digital hand atlas. Comput Med Imaging Graph 31(4–5):322–331
12. Thodberg HH, Kreiborg S, Juul A, Pedersen KD (2009) The BoneXpert method for automated determination of skeletal maturity. IEEE Trans Med Imaging 28(1):52–66
13. Tanner JM, Gibbons RD (1994) Automatic bone age measurement using computerized image analysis. J Ped Endocrinol 7:141–145
14. Brunk M, Ruppertshofen H, Schmidt S, Beyerlein P, Schramm H (2011) Bone age classification using the discriminative generalized hough transform. In: Handels H, Ehrhardt J, Deserno TM, Meinzer HP, Tolxdorff T (eds) Bildverarbeitung für die Medizin. Springer, Berlin, pp 284–288
15. Olabarriaga SD, Smeulders AWM (1997) Setting the mind for intelligent interactive segmentation: overview, requirements, and framework. In: Proceedings of IPMI, pp 417–422
16. Deserno TM (ed) (2011) Biomedical image processing, Chapter 11, Model-based segmentation. Springer, Berlin, pp 277–300. ISBN 978-3-642-15815-5
17. Aamodt A, Plaza E (1994) Case-based reasoning: foundational issues, methodological variations, and system approaches. AI Commun 7(1):39–59
18. Muller H, Michoux N, Bandon D, Geissbuhler A (2004) A review of content-based image retrieval systems in medical applications. Clinical benefits and future directions. Int J Med Inform 73(1): 1–23
19. Eakins JP, Graham ME (1999) Content-based image retrieval—a report to the JISC technology applications programme. Technical Report, Institute for Image Data Research, University of Northumbria at Newcastle, http://www.jisc.ac.uk/uploaded_documents/ jtap-039.doc Accessed 28 Jan 2010
20. Berner ES, McGowan JJ (2010) Use of diagnostic decision support systems in medical education. Methods Inf Med 49(4):412–417
21. Lehmann TM, Güld MO, Thies C, Fischer B, Spitzer K, Keysers D, Ney H, Kohnen M, Schubert H, Wein BB (2004) Content-based image retrieval in medical applications. Methods Inf Med 43(4):354–361
22. Güld MO, Thies C, Fischer B, Lehmann TM (2007) A generic concept for the implementation of medical image retrieval systems. Int J Med Inform 76(2–3):252–259

23. Güld MO, Thies C, Fischer B, Lehmann TM (2006) Content-based retrieval of medical images by combining global features, Lecturer notes in computer science, vol 4022, pp 702–711

24. Fischer B, Brosig A, Welter P, Grouls C, Guenther RW, Deserno TM (2010) Content-Based image retrieval applied to bone age assessment. In: Proceedings of SPIE, vol 7624, pp 121–130

25. Fischer B, Brosig A, Deserno TM, Ott B, Günther RW (2009) Structural scene analysis and content-based image retrieval applied to bone age assessment. In: Proceedings of SPIE, vol 7260, p 041-11

26. Zhang A (2007) A computer-aided-diagnosis (CAD) method combining phalangeal and carpal bone features for bone age assessment of children. Dissertation. University of Southern California

27. Deserno TM, Antani S, Long R (2009) Ontology of gaps in content-based image retrieval. J Digit Imaging 22(2):202–215

28. Muller H, Despont-Gros C, Hersh W et al (2006) Health care professionals' image use and search behaviour. In: Proceedings of MIE, pp 24–32

29. Hersh W, Muller H, Gorman P, Jensen J (2005) Task analysis for evaluating image retrieval systems in the ImageCLEF biomedical Image Retrieval Task. In: Proceedings of SOL, Portland, OR, USA

30. Deserno TM, Güld MO, Plodowski B, Spitzer K, Wein BB, Schubert H, Ney H, Seidl T (2008) Extended query refinement for medical image retrieval. J Digit Imaging 21(3):280–289

31. Deserno TM (ed) (2011) Biomedical image processing, Chapter 17, Digital imaging and communications in medicine. Springer, Berlin, pp 427–454. ISBN 978-3-642-15815-5

32. Welter P, Hocken C, Deserno TM, Grouls C, Günther RW (2010) Workflow management of content-based image retrieval for CAD support in PACS environments based on IHE. Int J Comput Assist Radiol Surg 5(4):393–400

33. Ruppertshofen H, Lorenz C, Schmidt S, Beyerlein P, Salah Z, Rose G, Schramm H (2011) Discriminative generalized hough transform for localization of joints in the lower extremities. J Comput Sci 26(1–2):97–105